

On-Line Sizing and Detection of Airborne Nanoparticles

Hiromu Sakurai

National Metrology Institute of Japan (NMIJ)

National Institute of Advanced Industrial Science and Technology (AIST)

2006 APEC Nanoscale Measurement Technology Forum

Taipei, Taiwan

September 27, 2006

Acknowledgements

AIST

Dr. Kensei Ehara (Group Leader)

Mr. Chih-Min Lin (visiting researcher from ITRI)

Dr. Yoshihiro Sato, Dr. Keiji Takahata

Dr. Keizo Saito, Dr. Akira Yabe, Ms. Emiko Onuma

Dr. Akio Iwasa (Electricity Standards Section)

Kanomax Japan, Inc.

RION Co. Ltd.

Funding

New Energy and Industrial Development Organization (NEDO)

Japanese Ministry of the Environment

Outline

Review on On-Line Measurement of Airborne Nanoparticles

- Measurement of Size Distribution by Scanning Electrical Mobility Spectrometer (SEMS)
- Sizing by Differential Mobility Analyzer (DMA)
- Detection by Condensation Nucleus Counter (CNC)
- Measurement of True Particle Mass by Aerosol Particle Mass Analyzer (APM)

Calibration of the Nanoparticle Measurement Instruments

- Size
- Concentration
- Monodispersity
- ISO Standardization Activity on DMA/SEMS

Review on On-Line Measurement of Airborne Nanoparticles

Size Distribution Measurement of Airborne Nanoparticles

Key Components

- Aerosol Charge Neutralizer Liu and Pui (1974)
- Differential Mobility Analyzer (DMA) Knutson and Whitby (1975a)
- Condensation Nucleus Counter (CNC) Agarwal and Sem (1980)

Scanning Electrical Mobility Spectrometer (SEMS) (Wang and Flagan (1992))

- Scanning Mobility Particle Sizer (SMPS™) (TSI, Grimm)
- Scanning Mobility Spectrometer (SMS™), part of WPS (Wide-range Particle Spectrometer) (MSP)



Grimm Aerosol Technik
(<http://www.grimm-aerosol.com>)



TSI
(<http://www.tsi.com>)



MSP
(<http://www.mspscorp.com>)

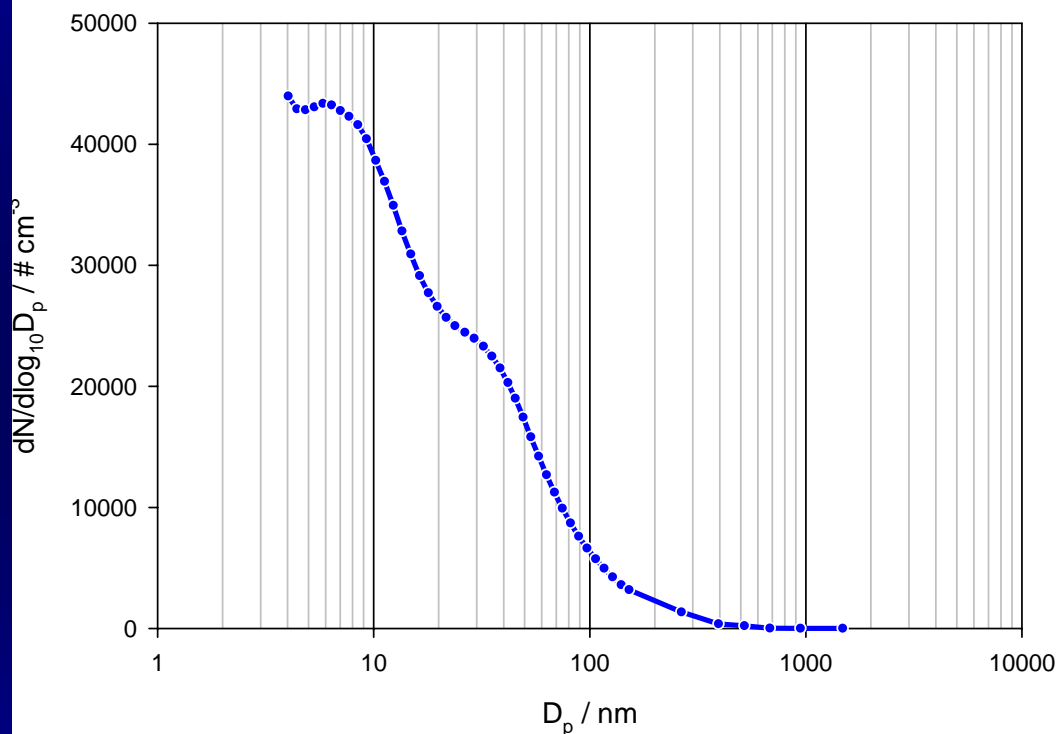
SEMS

- Measures the mobility-equivalent diameter
- Size range 3 – 1000 nm
- Accurate sizing
- High sizing resolution
- Time Resolution > 1 minute

- Considered to be the standard technique for size distribution measurement of airborne nanoparticles

Measurement of Airborne Nanoparticles

Average: $\sim 45,000$ particles/cm³



Annual Average Particle Size Distribution taken in St. Louis, Missouri, U.S.A. between April 2001 and April 2002

Particle Size Distribution Measurement System by the University of Minnesota



St. Louis Monitoring Station (A US EPA SuperSites Project)



Measurement of Airborne Nanoparticles

Size Distribution of Diesel Exhaust Particles

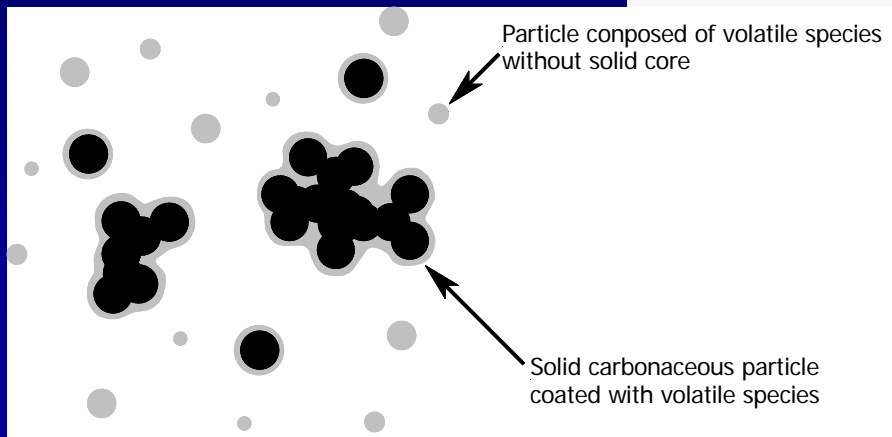
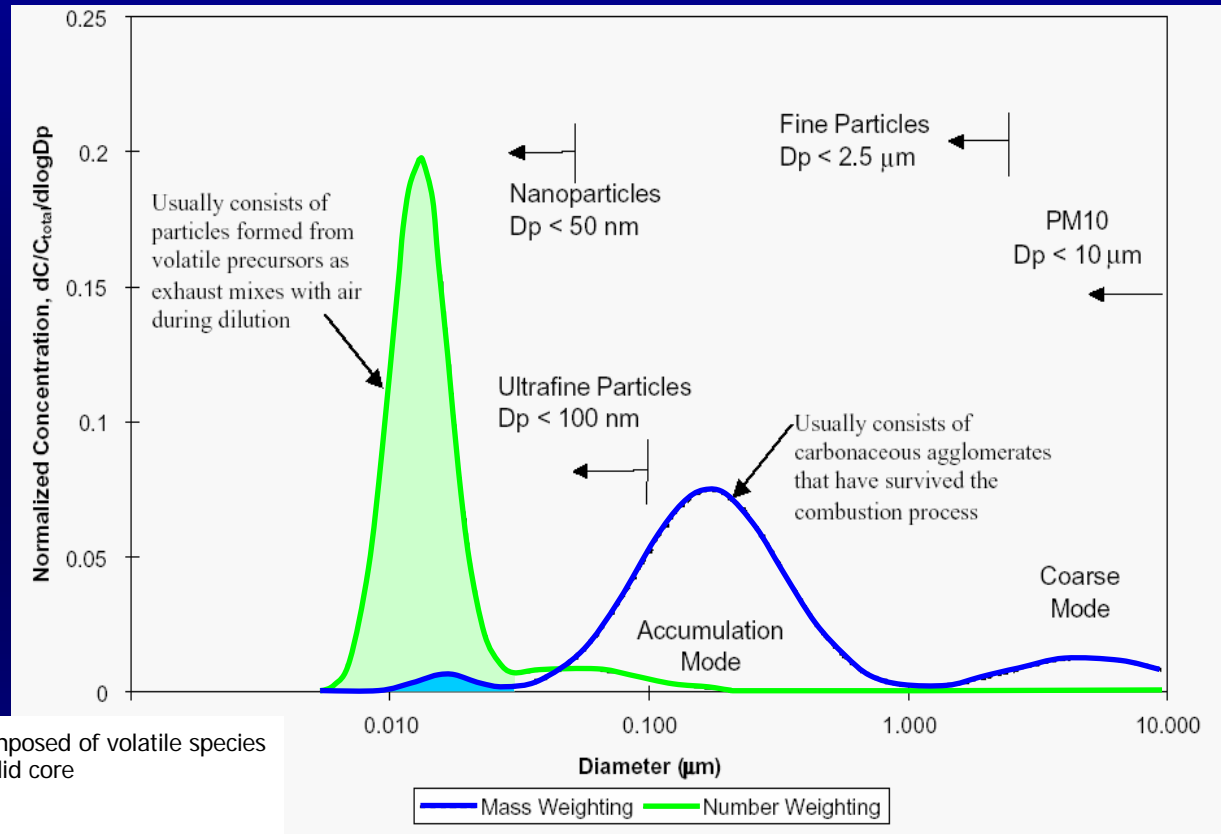
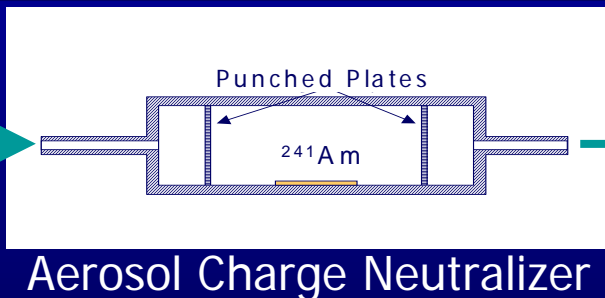


Figure taken from Kittelson (1998)

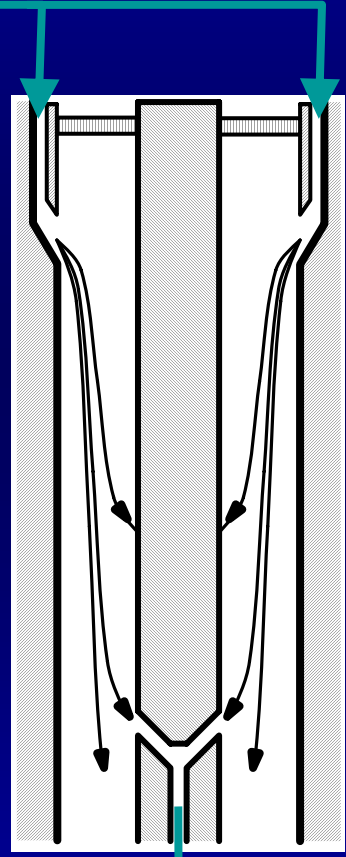
Cartoon image of diesel exhaust particles

SEMS

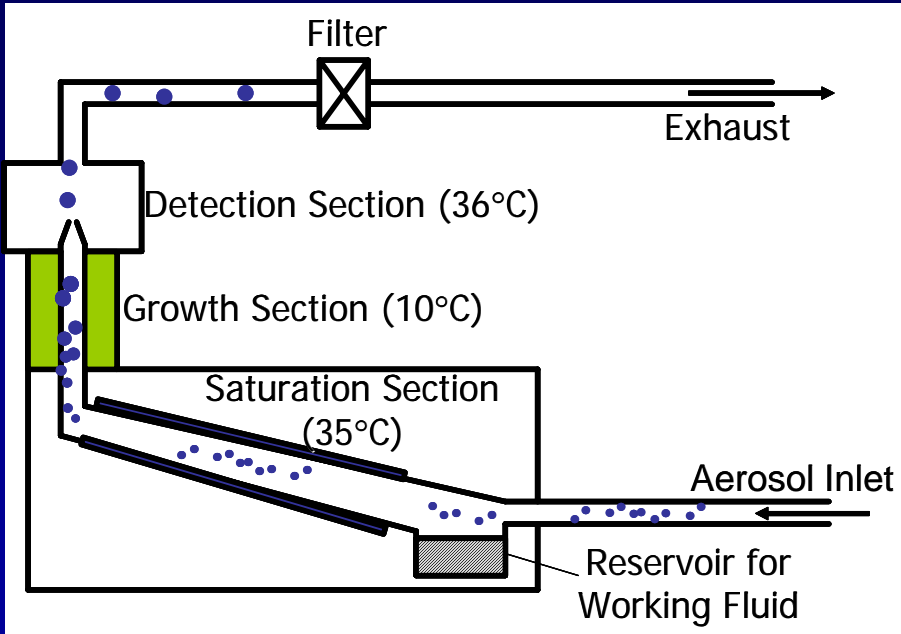
Aerosol to be Analyzed



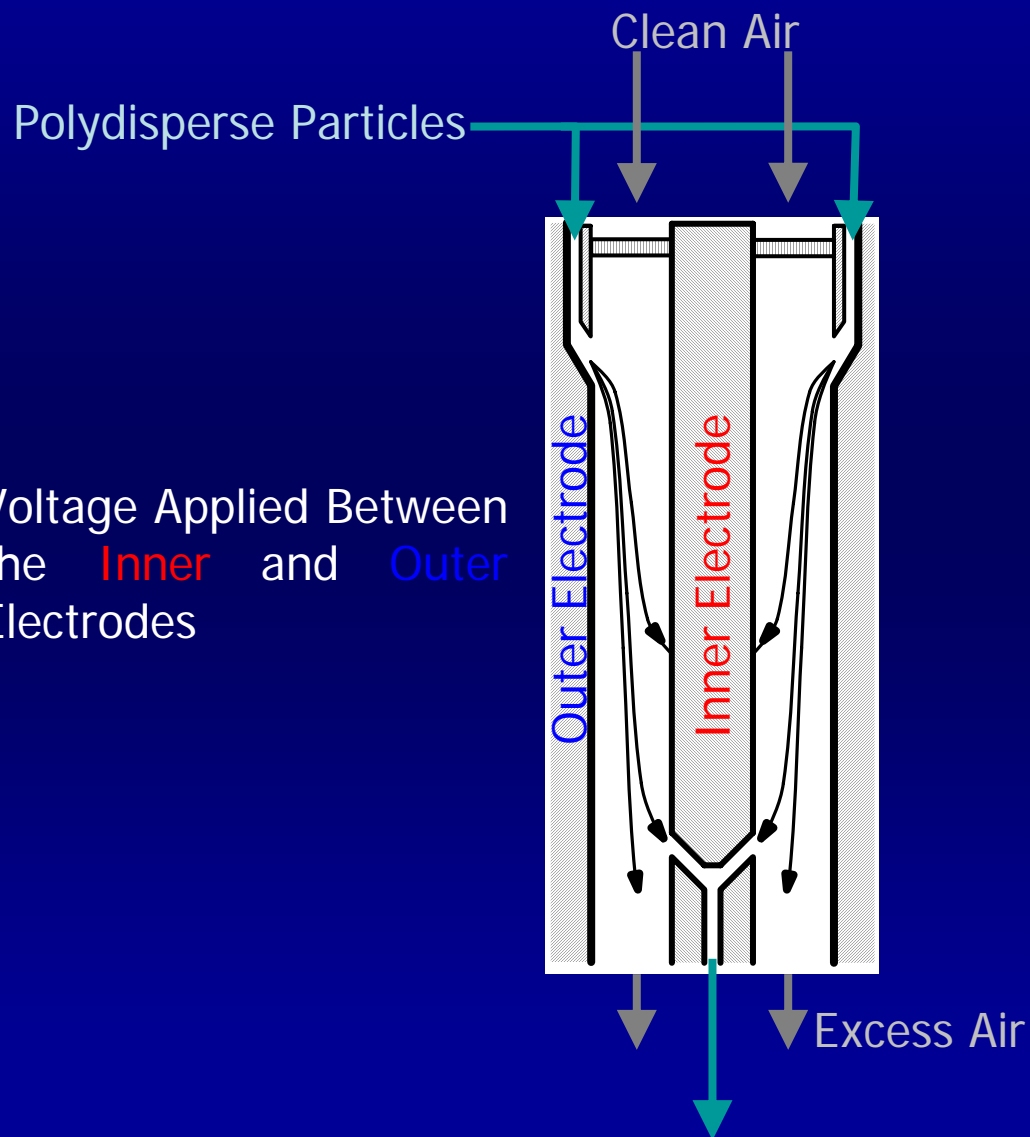
Differential Mobility Analyzer (DMA)



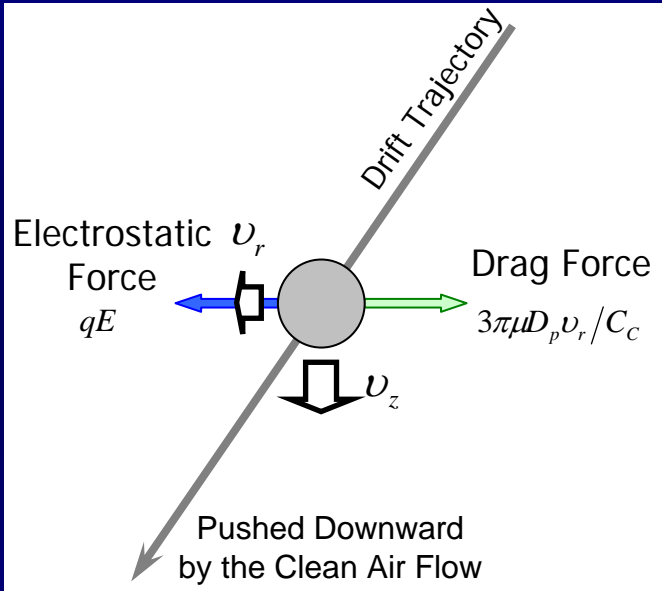
Condensation Nucleus Counter (CNC)



Differential Mobility Analyzer (DMA)



Voltage Applied Between the Inner and Outer Electrodes



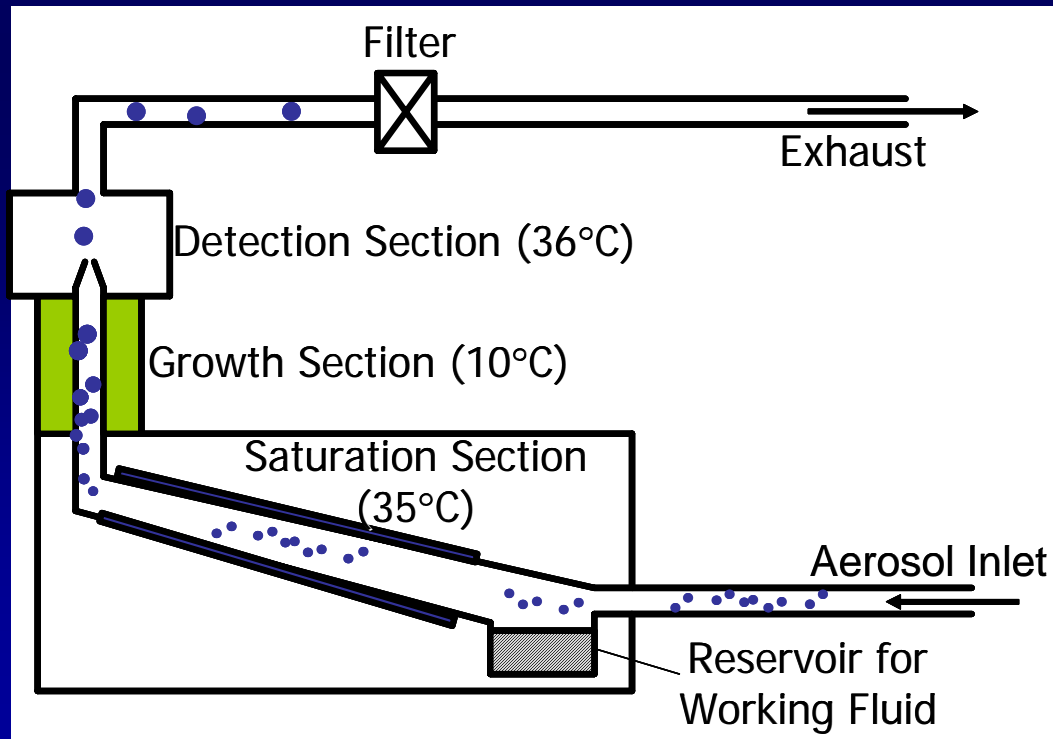
Particles in a Certain Electrical Mobility Band

Condensation Nucleus Counter (CNC)

Condensational Growth + Single Particle Counting

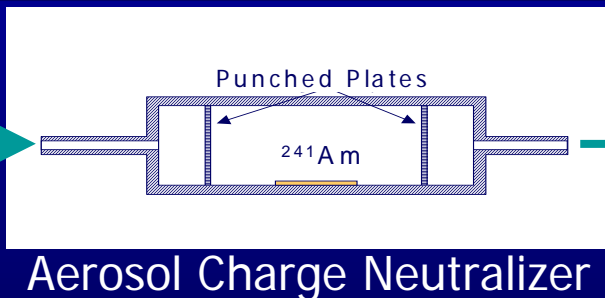


Accurate Determination of Particle Concentration Down to ~3 nm

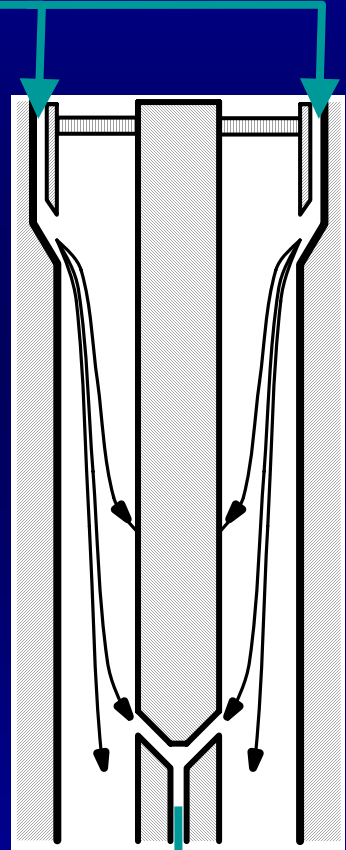


SEMS

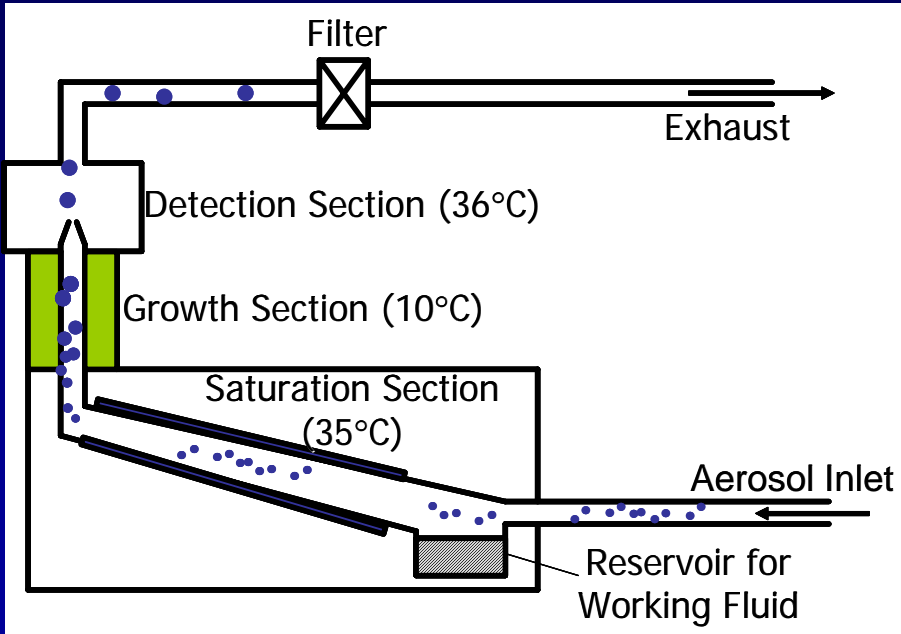
Aerosol to be Analyzed



Differential Mobility Analyzer (DMA)

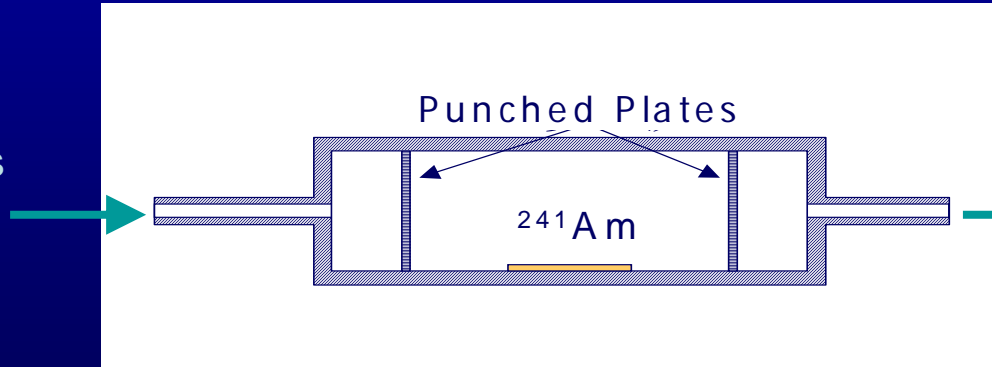


Condensation Nucleus Counter (CNC)



Aerosol Charge Neutralizer

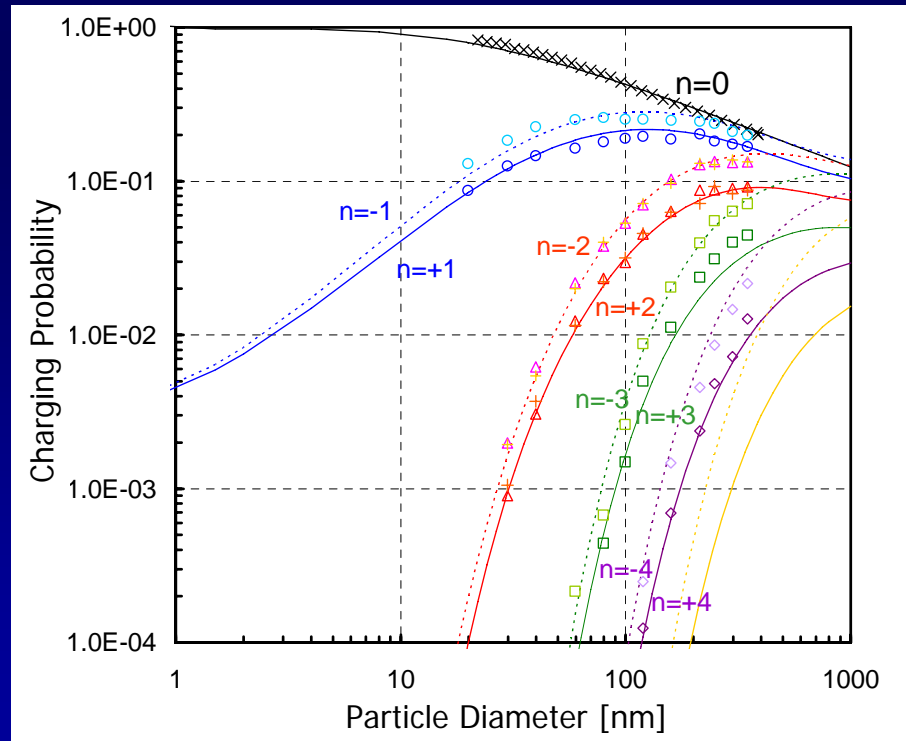
Aerosol Particles
of an Unknown
Charging State



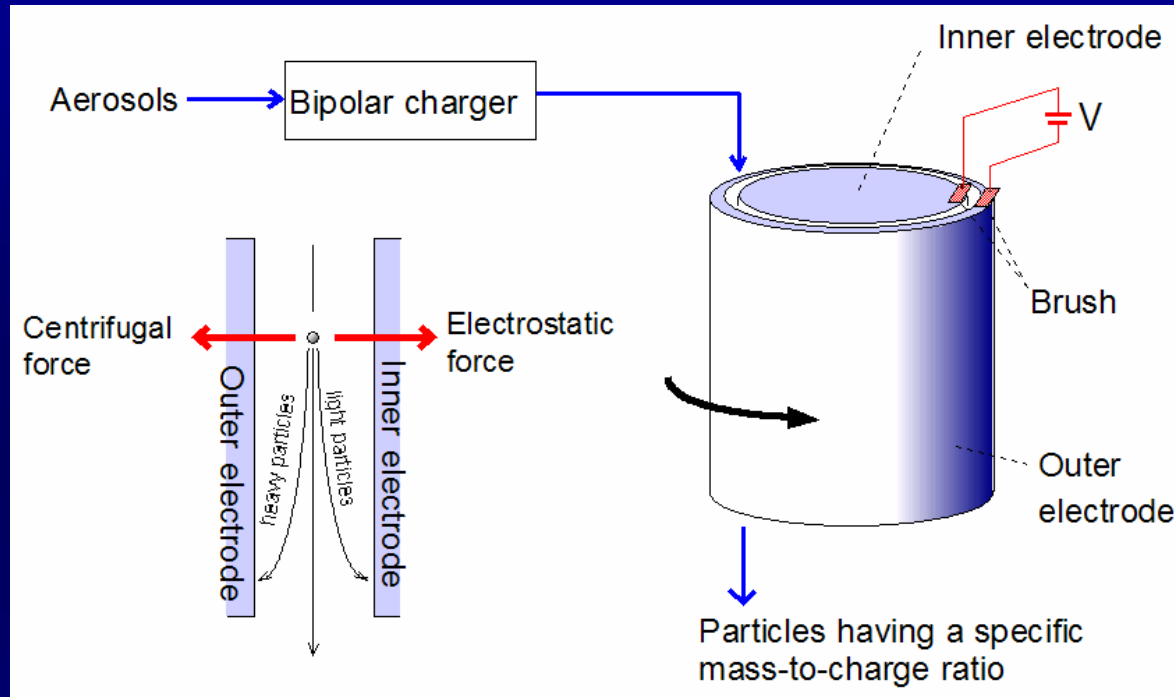
“Neutralized”
Aerosol Particles

“Reset” the charging state of incoming particles and impose the equilibrium charge distribution by reaction of bipolar ions with the particles.

The average of the charge distribution is zero (neutral).



Aerosol Particle Mass Analyzer (APM)



$$m = \frac{qV}{r_c^2 \omega^2 \ln(r_2 / r_1)}$$

m : particle mass

q : charge on the particle

r_1 : radius of the inner electrode

r_2 : radius of the outer electrode

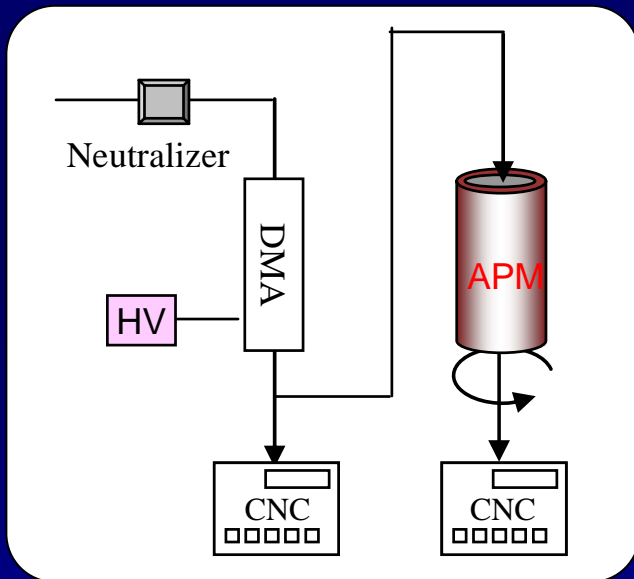
r_c : $(r_1 + r_2) / 2$

V : voltage between the two electrodes

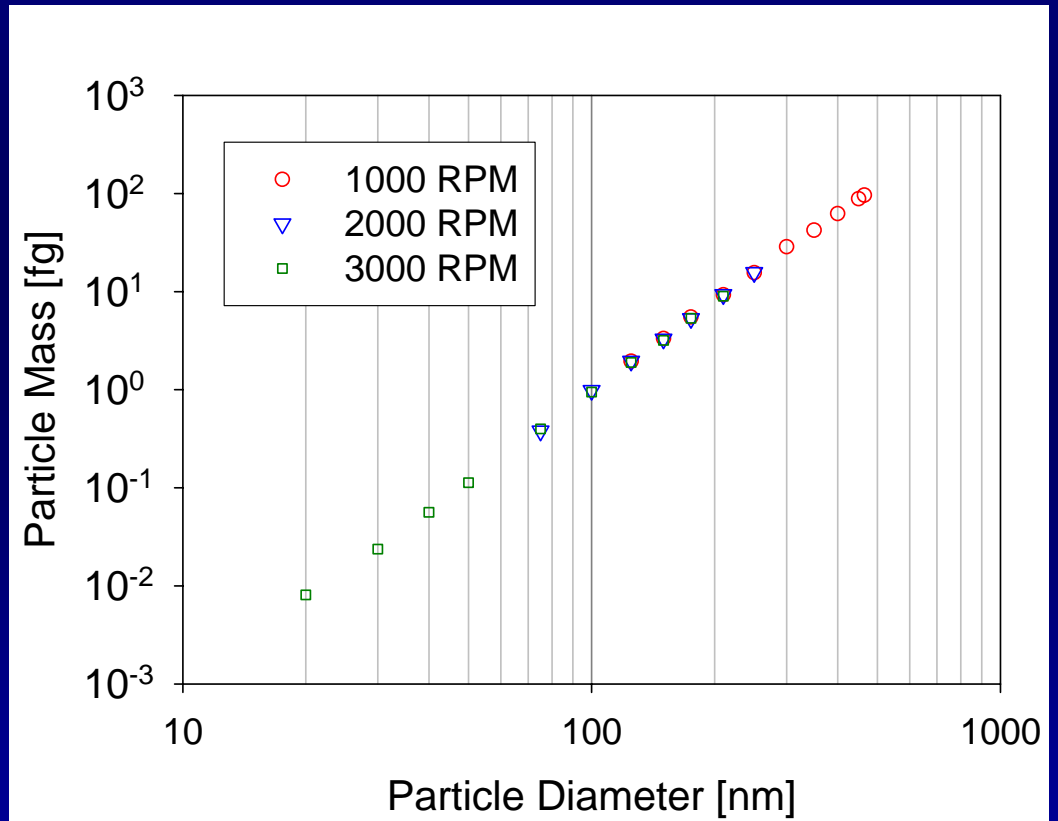
ω : rotation speed

APM Measurement of True Particle Mass

APM with DMA and CNCs



Mass of DMA-classified sodium chloride particles



Particle Shape by DMA & APM

The dynamic shape factor by DMA + APM (McMurry *et al.* 2000)

$$\chi = \frac{d_{me}}{d_{ve}} \cdot \frac{C_C(d_{ve})}{C_C(d_{me})}$$

$\chi = 1$ for spherical particles

$\chi > 1$ for non-spherical particles

ex. 1.08 for cube

1.15 for compact cluster of three spheres

d_{me} : Mobility-equivalent diameter (DMA)

d_{ve} : Volume-equivalent diameter (APM mass & material density)

C_C : Slip correction factor

Nanoparticles of Santovac[®] Oil

d_{me} [nm]	m_{true} [ag]	d_{ve} [nm]	χ [-]
25	8.95	24.2	1.06
39	35.6	38.4	1.03
63	160	63.3	0.99

Nanoparticles of Sucrose

d_{me} [nm]	m_{true} [ag]	d_{ve} [nm]	χ [-]
22	6.71	20.0	1.20
31	19.3	28.6	1.17
45	62.6	42.2	1.13

McMurry, P. H., Wang, X., Park, K., and Ehara, K. (2002). The relationship between mass and mobility for atmospheric particles: A new technique for measuring particle density, *Aerosol Sci. Technol.*, 36, 227-238.

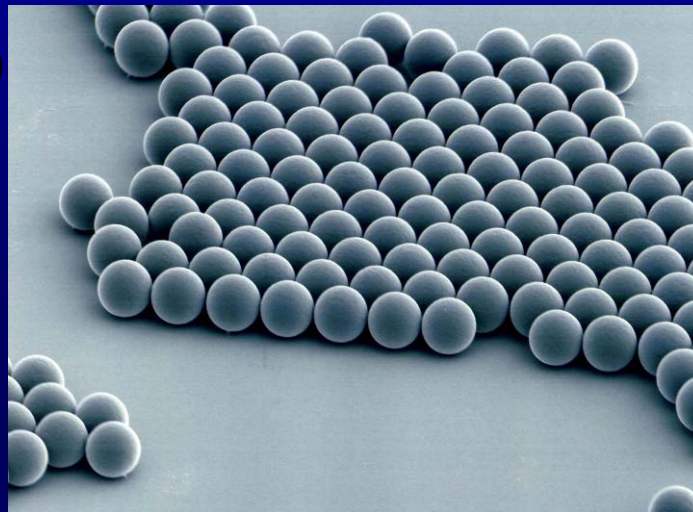
Calibration of the Nanoparticle Measurement Instruments

Particle Size

Particle Size Standard

Polystyrene Latex (PSL)

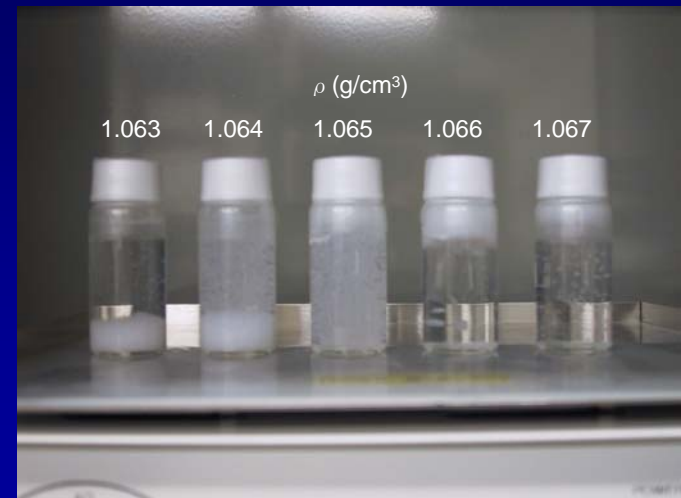
(Courtesy of JSR Corp.)



Determination of particle mass by the electro-gravitational aerosol balance method



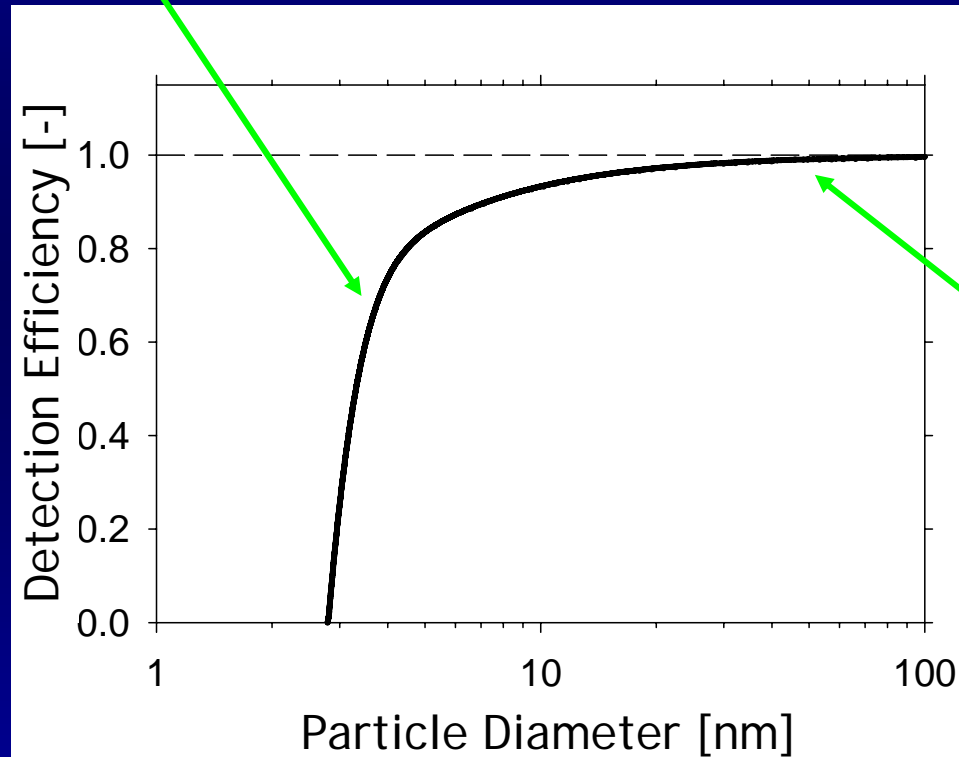
Determination of material density



Particle Concentration

Calibration of a CNC

Where does the detection efficiency drop?



Is the detection efficiency 100% at large particle sizes?

What about the linearity of the detection efficiency against the concentration?

Introduction

Japanese Primary Standard for Aerosol Particle Number Concentration

- Development underway at AIST
- Calibration standard for condensation nucleus counters (CNCs) and optical particle counters (OPCs)
- SI-traceable
- Service scheduled to begin in 2007

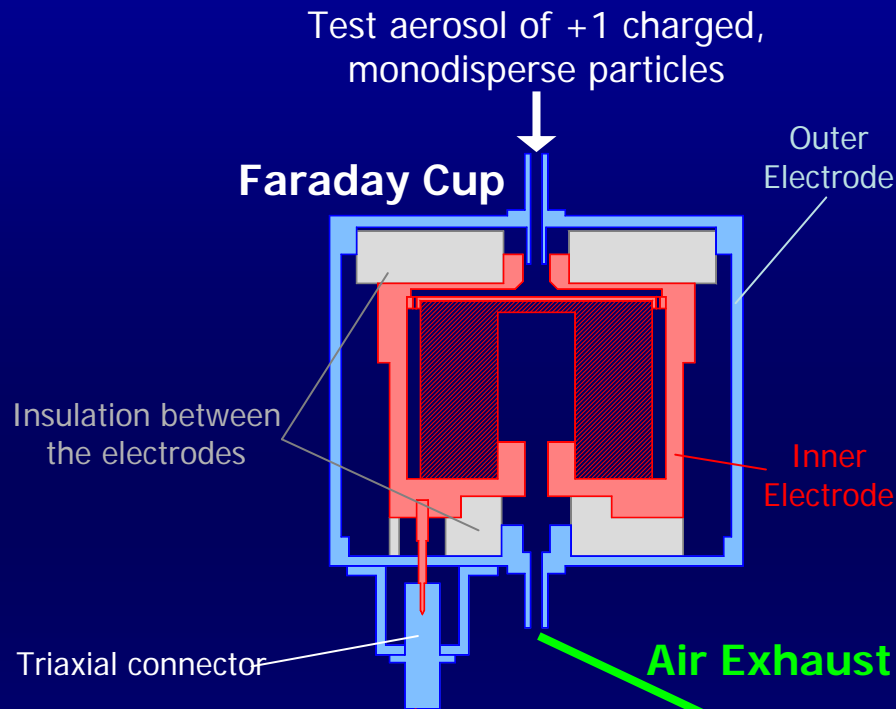
- Faraday-cup aerosol electrometer (AE) as the primary measurement instrument
 - AE has been most commonly used as a reference instrument in calibration of CNCs
 - The measurement principle and instrument structure are simple; important in evaluation of the measurement uncertainty.

Description of the Standard AE (1)

Three major components of the standard AE

- Faraday cup
- Electrometer
- Flow controller

$$N = \frac{I}{zeQ} \cdot \eta$$



Model 6430 Sub-femtoamp Remote Sourcemeter by Keithley Instruments, Inc.



Model MC-4000 Mass Flow Controller by Lintec Co. Ltd.

Description of the Standard AE (2)

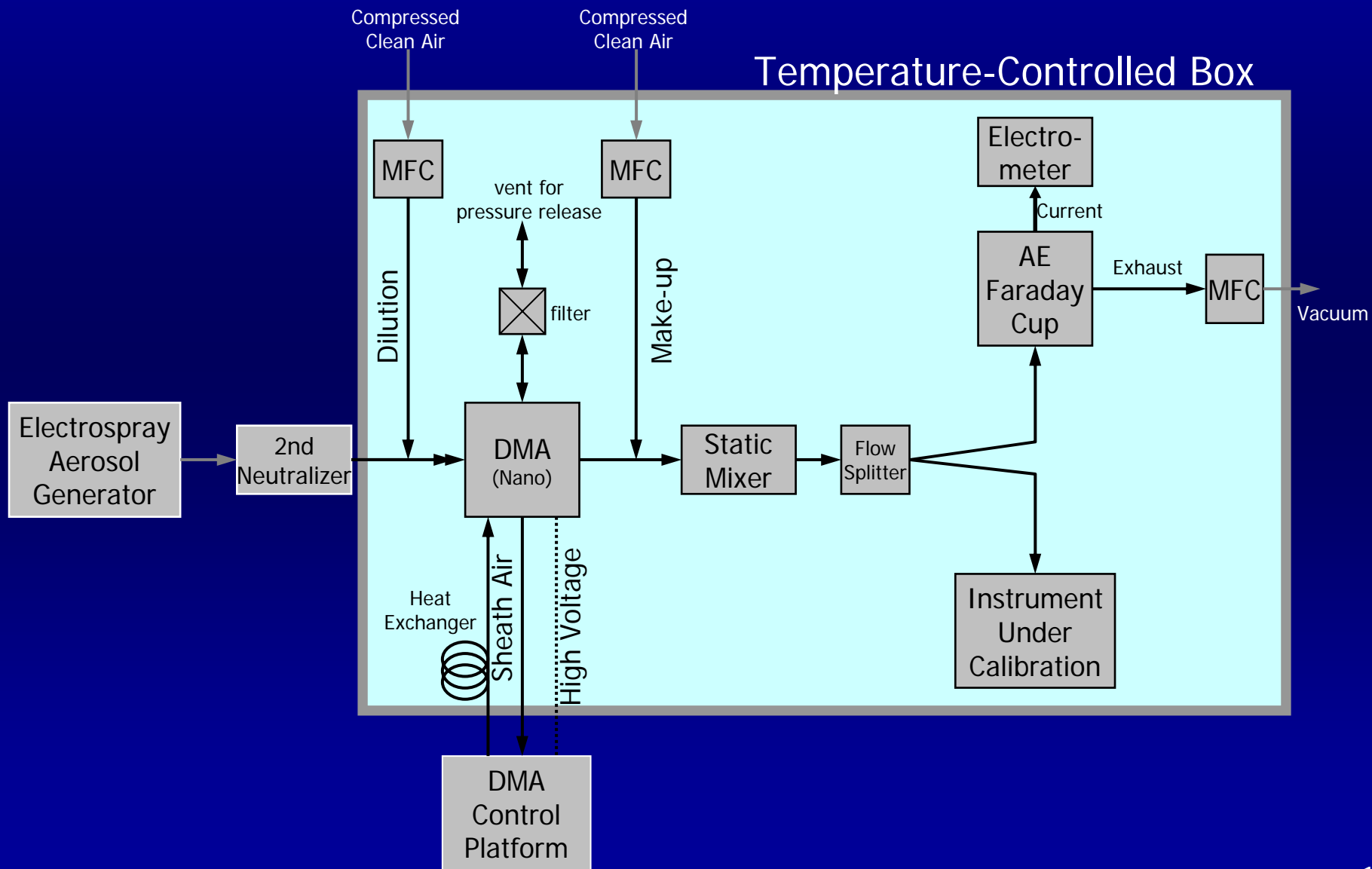
Keithley Model 6430 Sub-femtoamp Remote Sourcemeter

- Calibrated with NIST-traceable standards
- Measurement settings
 - 6 1/2-digit resolution; the last digit corresponds to 1 aA ($\text{aA} = 10^{-18} \text{ A}$)
 - Integration time of the A/D converter: 10 power-line cycles (highest accuracy)
 - 10-point repeat averaging filter turned on; Median and moving average filters off
- Data reporting interval: ~ 2.4 sec
- Current measurements are repeated at the above interval and measured data are recorded temporarily in the internal memory
- Measurement control and data acquisition from the internal memory was done through GP-IB with LabVIEW codes

Lintec Model MC-4000 Mass Flow Controller (Lintec Co. Ltd., Japan)

- Calibrated against a reference laminar flow meter that was calibrated with an NMIJ*- traceable standard
 - The reference flow meter manufactured by Sokken Co. Ltd., Japan
 - Laminar Flow Element LFE-27LM; Differential Pressure Transducer SDP-11; Output Voltage Amplifier SPX-D
 - 0.33% expanded uncertainty ($k = 2$) in the flow rate range of 5-27 L/min
- *NMIJ: National Metrology Institute of Japan

Calibration Facility Overview



Calibration Facility Details

- Temperature-controlled Box
 - A box of 90 cm x 90 cm x 90 cm provides a temperature controlled environment.
 - Internal temperature maintained at $\sim 23^{\circ}\text{C}$.
- Test aerosol generator (Sakurai *et al.*, 2006)
 - Electropray aerosol generator (TSI Model 3480)
 - Types of particles generated and their size range:
 - Polystyrene latex (PSL) 30, 50, 70, 100, 150, and 200 nm
 - Sucrose 5-50 nm
 - Santovac[®] oil 10-100 nm
 - The maximum concentration of $\sim 10^4$ particles/cc downstream of the DMA
 - Two Am-241 neutralizers used
- DMA for size-classification
 - The flow rate ratio of the sheath air to the aerosol is typically set at 10:1, but occasionally varied in the range between 3:1 and 20:1.
- Measurement control and data acquisition are computerized with National Instruments DAQ devices and LabVIEW codes.

Determination of Particle Concentration by AE and Factors That Contribute to Uncertainty

$$N = \frac{I}{zeQ} \cdot \eta$$

- N Particle number concentration [particles/cc]
- I Current [A]
- z Average number of charges per particle [-]
- e Elementary charge (1.602×10^{-19} C)
- Q Volumetric flow rate [cm^3/s]
- η "Faraday cup efficiency"

"Faraday cup efficiency": The ratio of the number of particles detected by the AE to that of particles which enters into the inlet of the AE. When all entered particles are detected (the ideal case), this value is unity. This takes into account all non-ideality of the Faraday cup in concentration measurement. This is the only parameter in the equation above that is particle size dependent.

The Law of Propagation of Uncertainty

$$u_c^2(N) = \left(\frac{\partial N}{\partial I}\right)^2 u^2(I) + \left(\frac{\partial N}{\partial z}\right)^2 u^2(z) + \left(\frac{\partial N}{\partial e}\right)^2 u^2(e) + \left(\frac{\partial N}{\partial Q}\right)^2 u^2(Q) + \left(\frac{\partial N}{\partial \eta}\right)^2 u^2(\eta)$$

$u_c(N)$

Combined standard uncertainty of N

$u(I), u(z), u(e), u(Q), u(\eta)$

Standard uncertainty of $I, \eta, z,$ and Q

$\frac{\partial N}{\partial I}, \frac{\partial N}{\partial e}, \frac{\partial N}{\partial z}, \frac{\partial N}{\partial Q}, \frac{\partial N}{\partial \eta}$

Partial derivatives ("sensitivity coefficients")

AIST Source of Uncertainty of the Standard AE:

$$u(Q), u(z), u(e), \text{ and } u(\eta)$$

- The standard uncertainty of Q is estimated to be 1% of the flow rate.
- Uncertainty of z is estimated to be zero.
- Uncertainty of e is considered negligible.
- Uncertainty of η is under evaluation. Two factors are considered to contribute:
 - Filter efficiency: This was experimentally determined with 100-nm NaCl particles and evaluated to be >99.99% at the flow rates of 1-10 L/min.
 - Losses in the inlet tube: Direct experimental determination of this factor has not been carried out. The theory for diffusional deposition predicts that losses are negligibly small at particle sizes above 20 nm at 1 L/min of the sampling flow rate.

Under conditions when η is nearly unity, the uncertainty is considered negligible.

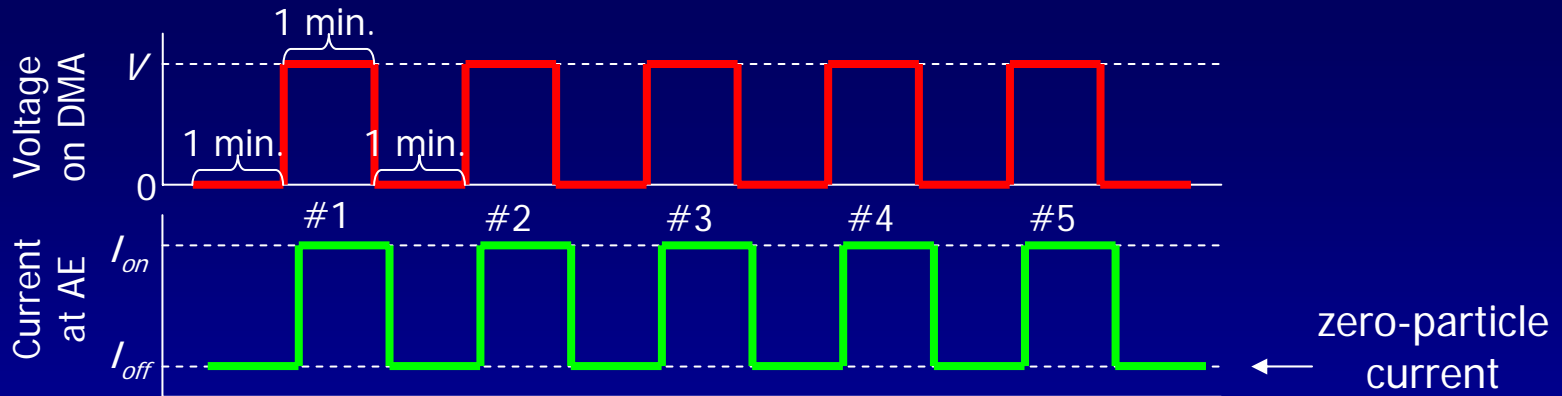
Source of Uncertainty of the Standard AE: $u(I)$

- Measurement of very low current can be affected by the fluctuation of the environment temperature. By housing the AE in the temperature-controlled box, the drift of the current reading, recorded without feeding test aerosol into the FC (zero-particle current), was suppressed significantly.
 - The standard deviation of the temperature fluctuation in the box is about 0.1°C.
- The offset term in the current uncertainty was reevaluated.
 - An article by Keithley Instruments Inc. (Daire 2005) discusses how to reduce the uncertainty for measurement of current of atto-amperes. It recommends measurement of the net current, i.e., the current difference between the “on” and “off” states.
 - The “on” and “off” states are produced by turning on and off the voltage on the DMA.

Source of Uncertainty of the Standard AE: $u(I)$

(continued)

- The interval of the on/off switching needs to be optimized: the longer interval allows more averaging for current measurement in each interval, which reduces error due to random noise; on the other hand, the longer interval increases the drift of the zero-particle current, which increases measurement uncertainty. Multiple repetition of on/off switching with a short interval balances the two factors.
- Currently a procedure of 5-fold repetition of on/off switching at 1-minute interval is being tested.

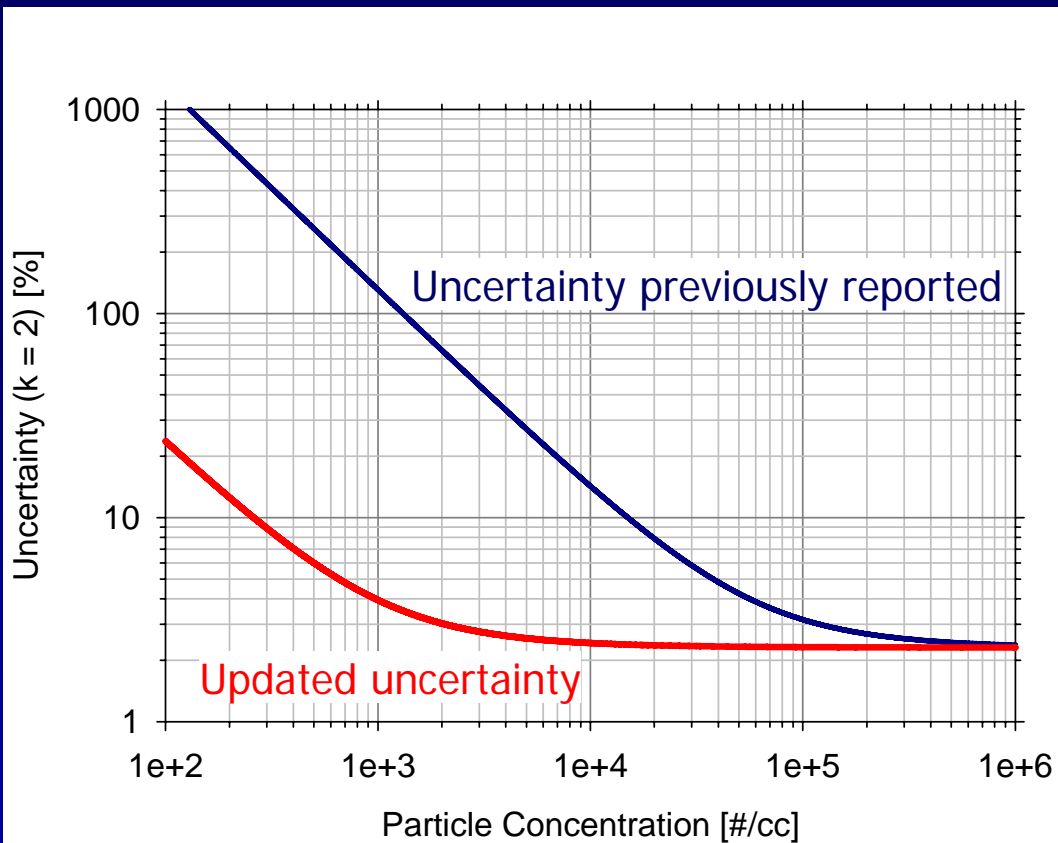


- The standard uncertainty due to the drift of zero-particle current by this procedure was experimentally evaluated to be 0.03 fA.
- The updated standard uncertainty of I : $u(I) [\text{fA}] = 0.006I + 0.03$

Combined Uncertainty of the Standard AE

Approximated combined standard uncertainty

$$u_c(N) \cong \sqrt{\left(\frac{\partial N}{\partial I}\right)^2 u^2(I) + \left(\frac{\partial N}{\partial Q}\right)^2 u^2(Q)}$$



The combined uncertainty was calculated by including only the uncertainties of current and flow rate for the case of 1.0 L/min.

The expanded relative uncertainty (k=2) decreased from 14% to 2.5% at 10⁴ particles/cc. The expanded uncertainty at 10³ particles/cc is 4%, which indicates that the AE is acceptable as the standard at this concentration.

Uncertainty in Calibration

The following lists additional factors that must be considered in evaluating the uncertainty in calibration of an instrument (e.g., CNC) using the standard AE:

- Uncertainty of measurement by the standard AE (discussed above)
- Uncertainty in splitting ratio at the flow splitter
- Uncertainty in difference in losses in the tubes after the flow splitter
- Variation of concentration due to instability of the test aerosol generator
- Scattering of concentration readings measured by the instrument under calibration

Comparison to OPC

Comparison of the standard AE with an OPC underway

- Comparison between two instruments of different measurement principles is expected to provide important information on the accuracy of both instruments.



RION Model KC-22B
Optical Particle Counter

The OPC: RION Model KC-22B (RION Co. Ltd., Tokyo, Japan)

- Modified by the manufacture upon our request to increase the maximum measurable concentration (5% coincidence losses) to 10^3 particles/cc from 10^2 particles/cc of the original configuration
- A mass flow meter (Lintec Model MM-3000) was added for monitoring the flow rate.
- Intended to be part of the next-generation primary standard that covers concentrations below 10^3 particles/cc.

Preliminary results of comparison experiment with 150-nm PSL particles suggest that the agreement between the standard AE and OPC is good.

Monodispersity

Introduction

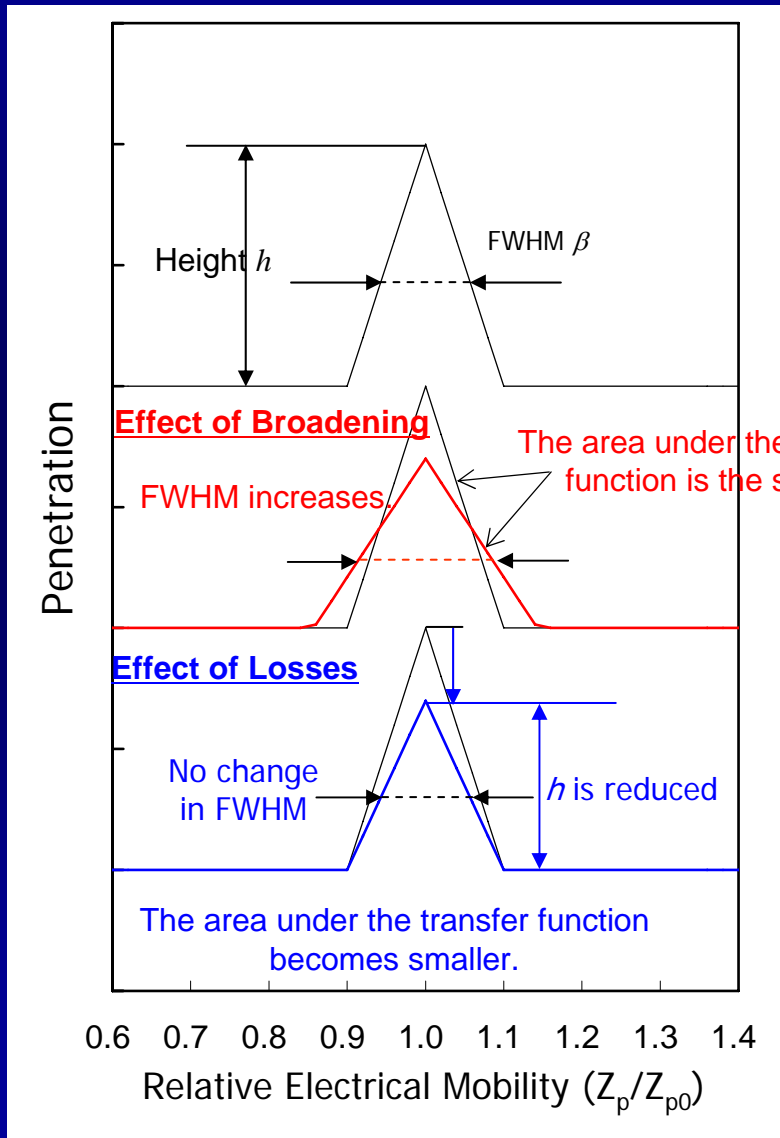
Standard for calibration of monodispersity of DMA size classification

- Measurement by a DMA of quasi-monodisperse polystyrene latex (PSL) particles of a known size distribution would provide information on the monodispersity of DMA classification.
- A DMA of which the transfer function is carefully characterized is needed.

Experimental evaluation of the transfer function is a difficult task.

- Martinsson *et al.* recently reported a method to determine the non-ideality of the transfer function. (Martinsson *et al.*, 2001).
- We improved their method and applied it to evaluate three pairs of a TSI 'Long' DMA and controller platform, which are the most widely used DMAs.

The Broadening and Loss Parameters Defined by Martinsson *et al.* (2001)



Ideal Transfer Function

The transfer function has a triangular shape. (It is assumed that the flow rates of incoming and outgoing aerosol flows are identical.) In the relative electrical mobility scale,

$$FWHM : \beta = \frac{Q_a}{Q_s}$$

$$Height : h = 1$$

Non-Ideal Transfer Function

It is assumed that the shape is still triangular. The following two parameters add non-ideality:

μ : the broadening parameter $0 \leq \mu \leq 1$

λ : the loss parameter $0 \leq \lambda \leq 1$

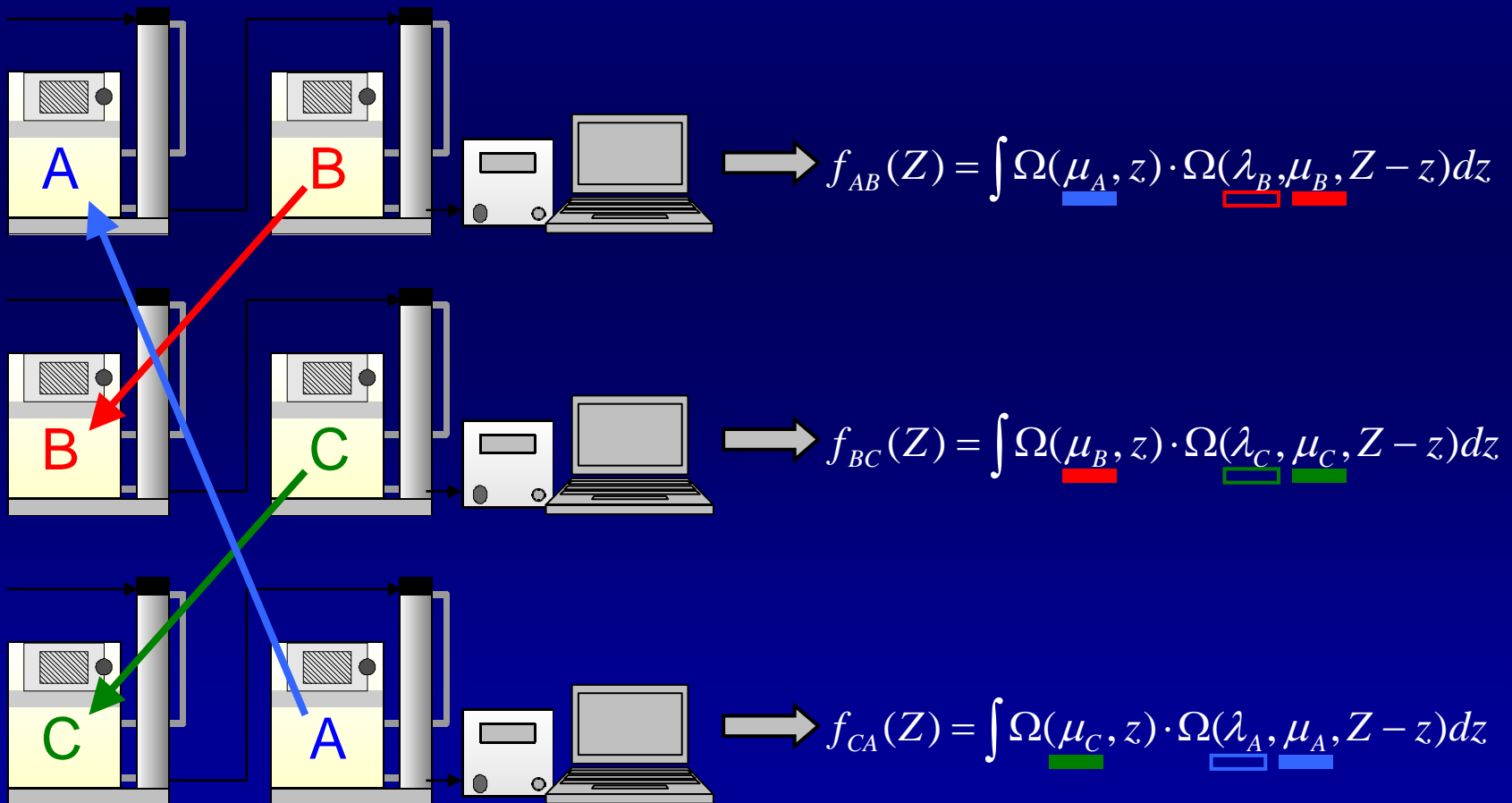
$$\beta = \frac{Q_a}{Q_s} \cdot \frac{1}{\mu}$$

$$h = \mu \lambda$$

When the parameters are unity, the transfer function is identical to the ideal one, i.e., no broadening or losses.

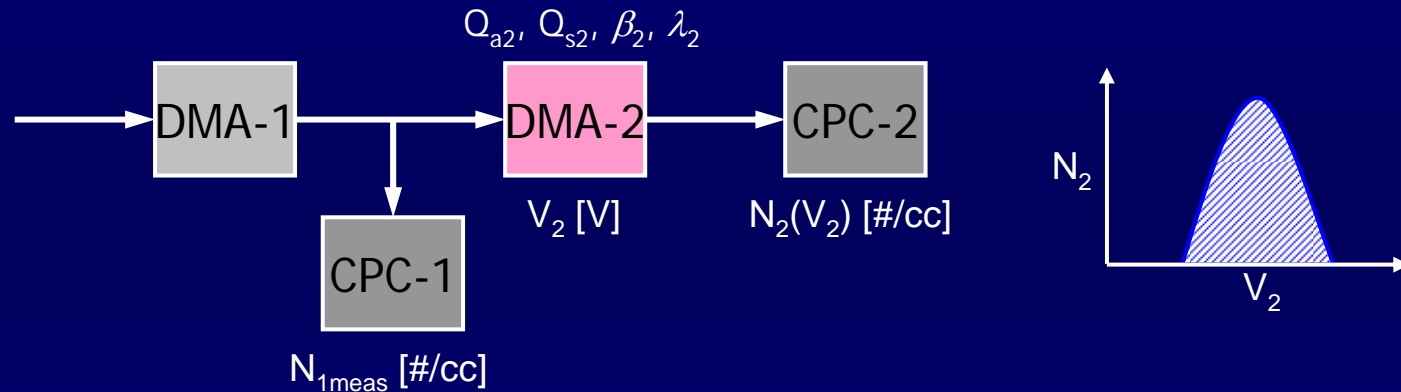
Triple Tandem DMA Measurements

Based on the procedure by Martinsson et al. (2001), three sets of tandem DMA measurements are taken. Total of six parameters, i.e., three broadening (μ_A, μ_B, μ_C) and three loss ($\lambda_A, \lambda_B, \lambda_C$) parameters, are initially unknown.



Determining the Loss Parameter

Determination of the loss parameter follows the method by Martinsson *et al.* (2001). For each tandem DMA measurement, the loss parameter of the downstream DMA (DMA-2), λ_2 , is obtained.

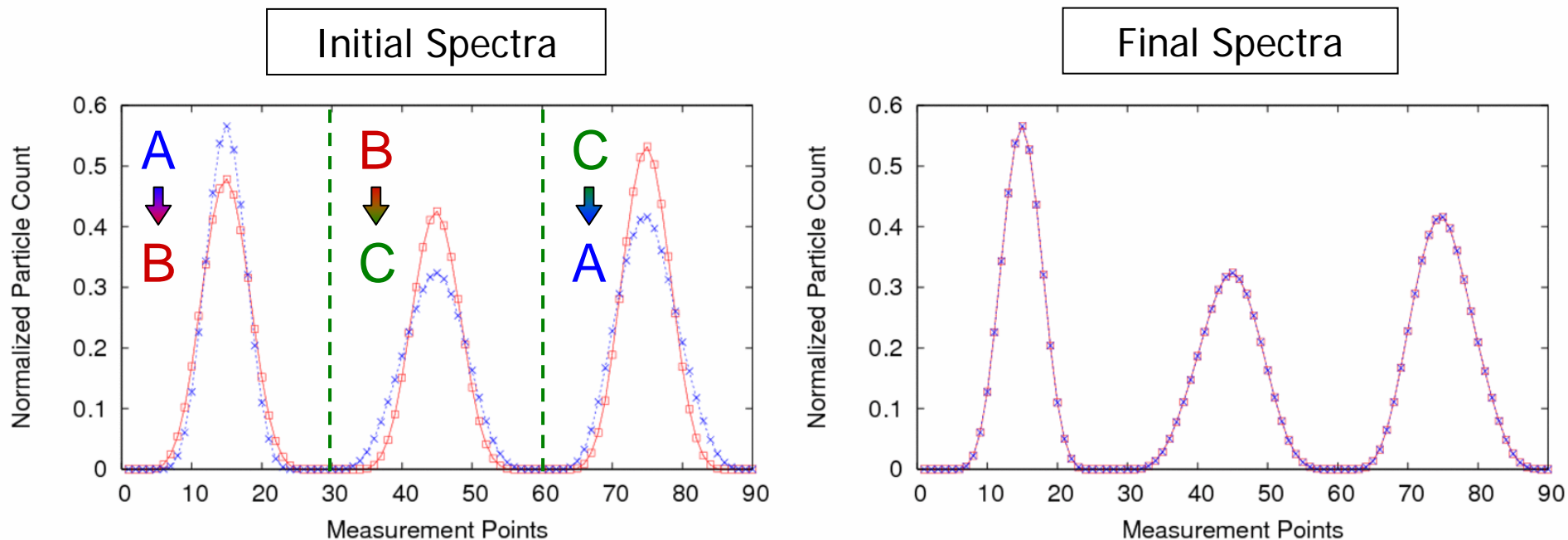


- Derivation of N_{1calc} from the $N_2(V_2)$ - V spectrum data using β_2 and λ_2 is based on the method by Knutson and Whitby (1975b).
- The loss parameter of DMA-2, λ_2 , can be described with $M_{1meas}, N_2(V_2), V_2, Q_{a2}, Q_{s2}$, and β_2 by equating N_{1calc} above and N_{1meas} and solving for it. The initial assumption of $g(\beta_2)=1$ is to be revised once μ_2 (hence β_2) is obtained.

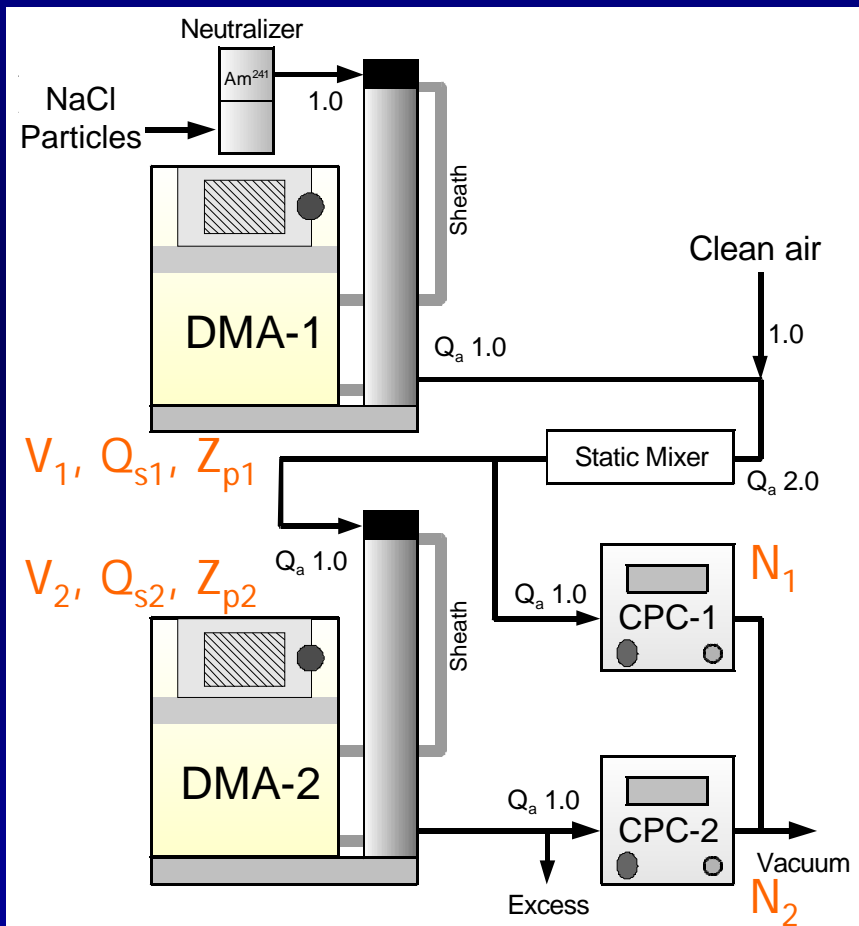
Determining the Broadening Parameter

The procedure to determine the broadening parameter was similar to the method by Martinsson *et al.* (2001). Once the loss parameters of the three DMAs were determined, the $N_2/N_1-Z_{p2}/Z_{p1}$ spectra from the three tandem DMA measurements were simultaneously fitted with the three broadening parameters. The fitting calculation was done using the Leasqr function in the Octave Toolbox, a non-linear least square fitting code by the Levenberg-Marquardt method.

We added a modification to the method by Martinsson *et al.*, which is discussed later.



Experimental Setup and Procedure



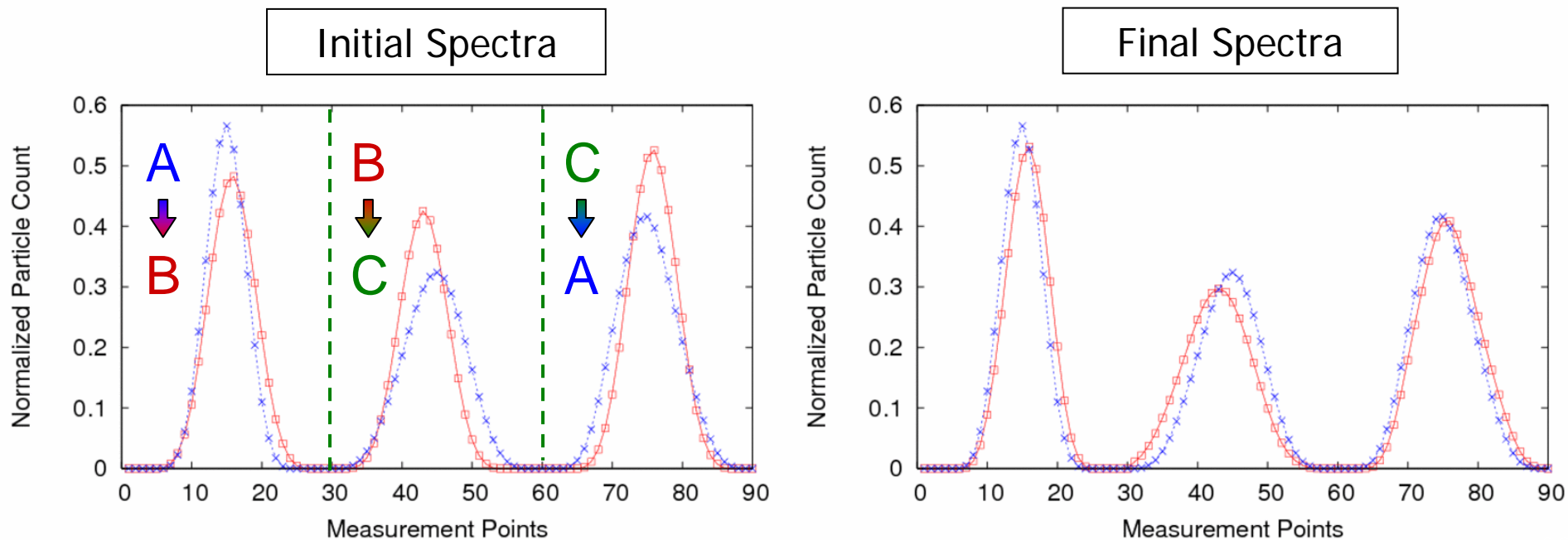
- In the study by Martinsson *et al.* (2001), only the DMA column was the objective of the analysis, and the DMA controlling parts (i.e., high voltage power supply + sheath air generator) were not included in the evaluation. This is suitable when comparison of different columns is the main purpose of the study.
- On the other hand, we treated the set of a DMA and a controller as an inseparable system. We think this will more likely be the case when a DMA is brought in to our lab for calibration.
- Three sets of TSI DMAs (Model 3081 'Long' DMA column + Model 3080 DMA Controller Platform) were used in our study:

Set	DMA Column	DMA Controller
A	S/N 70446038	S/N 70447130
B	70517084	70505245
C	70517087	70532112

Modified Analytical Method (1)

We noticed that very small errors in sheath air flow rates, which may occur in flow rate calibration, affect results of the fitting calculation significantly.

A model fitting calculation demonstrated that errors of 0%, +2%, and -2% assumed for DMA-A, DMA-B, and DMA-C, respectively, resulted in the broadening parameters $(\mu_A, \mu_B, \mu_C) = (1.18, 0.74, 0.48)$ while the correct values were $(1.00, 0.90, 0.50)$.

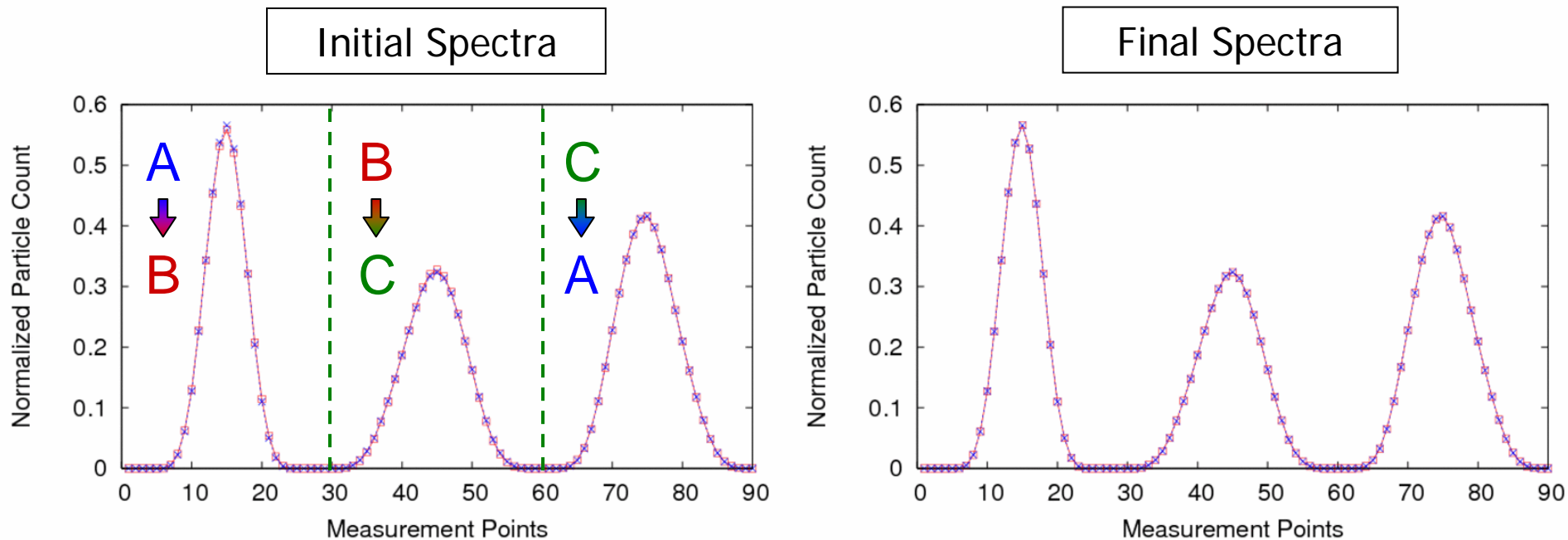


Modified Analytical Method (2)

A step to adjust sheath air flow rates was added to correct errors in sheath air flow rates.

This was done by running an additional fitting calculation with three sheath air flow rates and three broadening parameters (total six) as the fitting parameters.

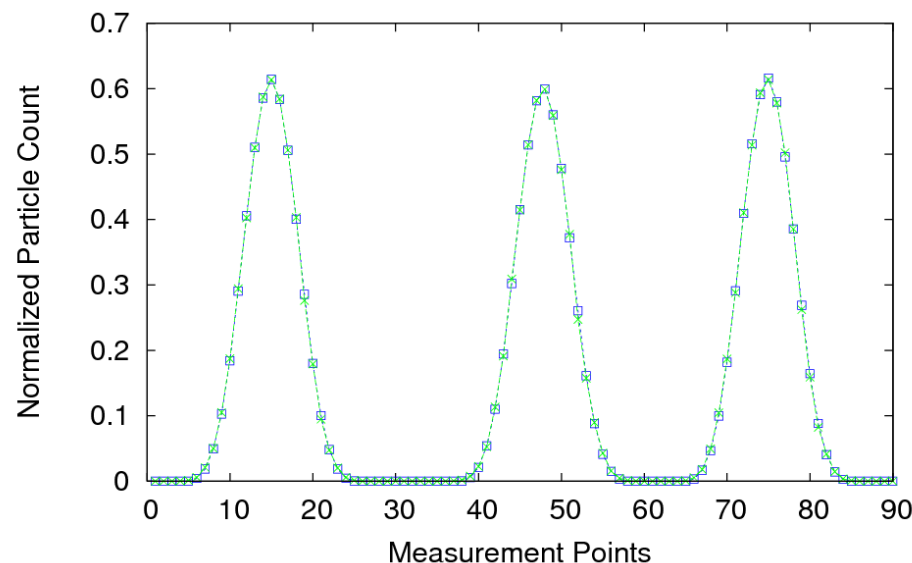
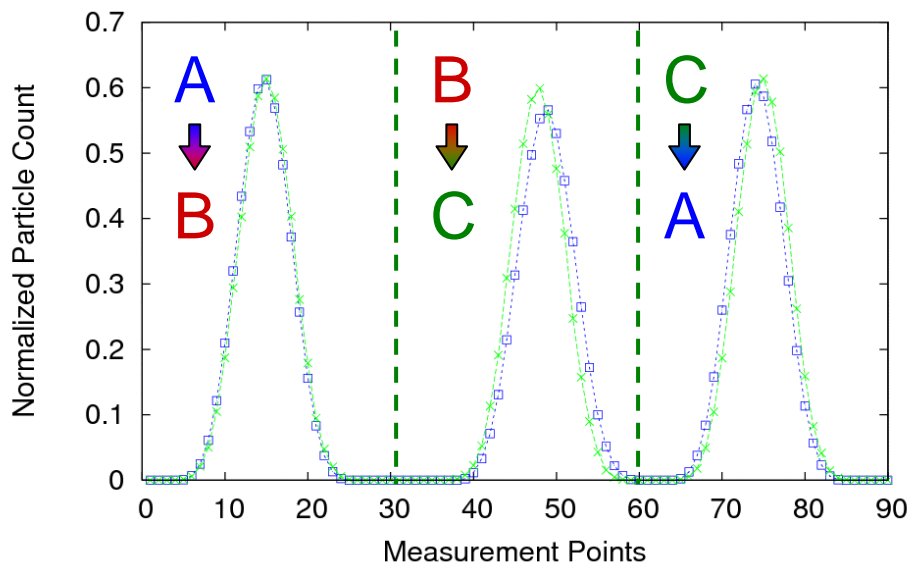
Since the sheath air flow rates were updated after the six parameter fitting, the loss parameters must be reevaluated, which affects the values of the broadening parameters. Therefore, after recalculating the loss parameters, another fitting calculation of the broadening parameter is needed.



Analysis of Actual Data by the Modified Method

Example of analysis of actual experimental data by the modified method

- DMA sheath air flow rates measured as 14.93, 14.71, and 15.27 L/min for DMA-A, DMA-B, and DMA-C, respectively (Aerosol flow rate 1.0 L/min)
- $(\lambda_{A_i}, \lambda_{B_i}, \lambda_{C_i}) = (0.92, 0.92, 0.93)$ and $(\mu_{A_i}, \mu_{B_i}, \mu_{C_i}) = (1.05, 0.94, 0.91)$ if analyzed by the original procedure by Martinsson *et al.* (2001).
- The flow rates were corrected to 14.98, 14.80, and 15.17 L/min, and the loss and broadening parameters were calculated as $(\lambda_{A_i}, \lambda_{B_i}, \lambda_{C_i}) = (0.92, 0.93, 0.93)$ and $(\mu_{A_i}, \mu_{B_i}, \mu_{C_i}) = (1.00, 0.97, 0.99)$ with the modified method.
- Note that the corrections of the flow rates were very small, i.e., less than 1%, and the errors in the broadening parameter were nearly 10%.



Experimental Conditions

Measurement on the flow-rate ratio dependence

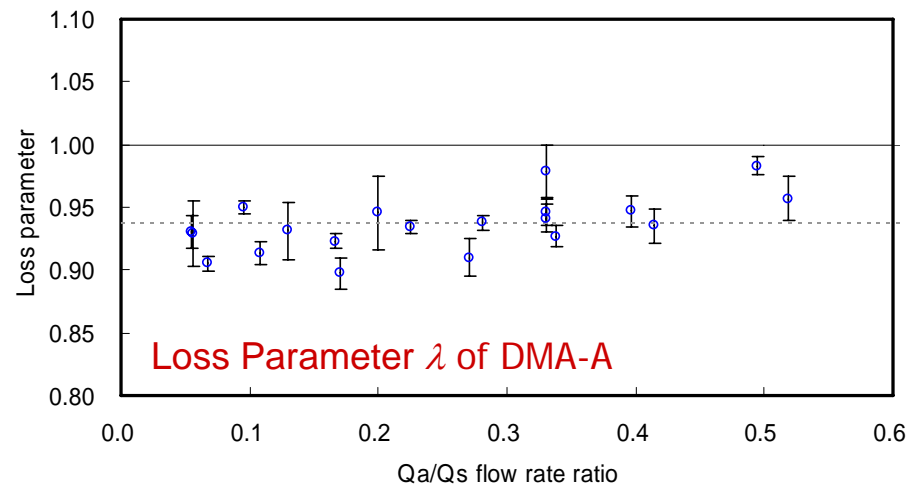
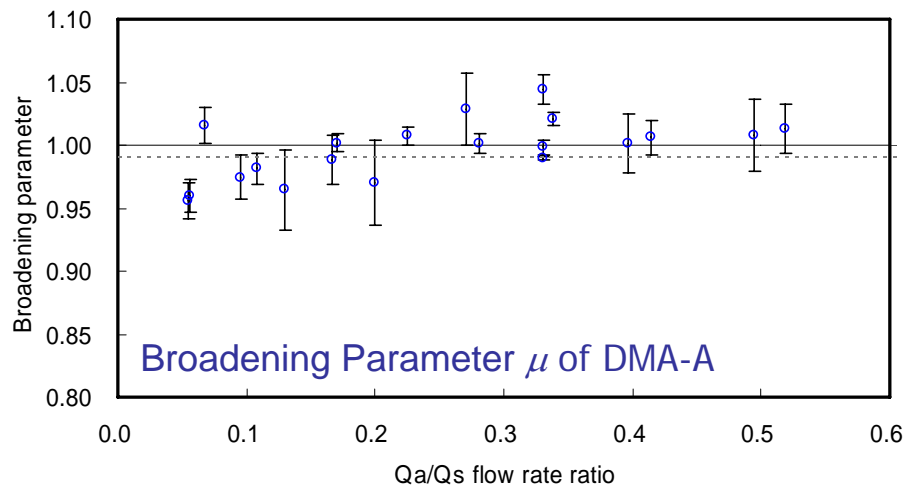
- Measurements were done at 100 nm.
- The flow-rate ratio is defined as Q_a/Q_s , where Q_a and Q_s are the aerosol and sheath-air flow rates, respectively.
- Flow-rate ratios between 0.05 and 0.5 were investigated. The aerosol flow rate (Q_a) was varied between 1.0 and 6.0 L/min, and the sheath air flow rate (Q_s) was varied between 2.0-18.0 L/min.

Measurement on the particle size dependence

- The sheath air flow rate was set at either 10 or 18 L/min. The aerosol flow rate was fixed at 1.0 L/min.

To investigate the repeatability, three sets of measurements were carried out in a single day under the same experimental setting.

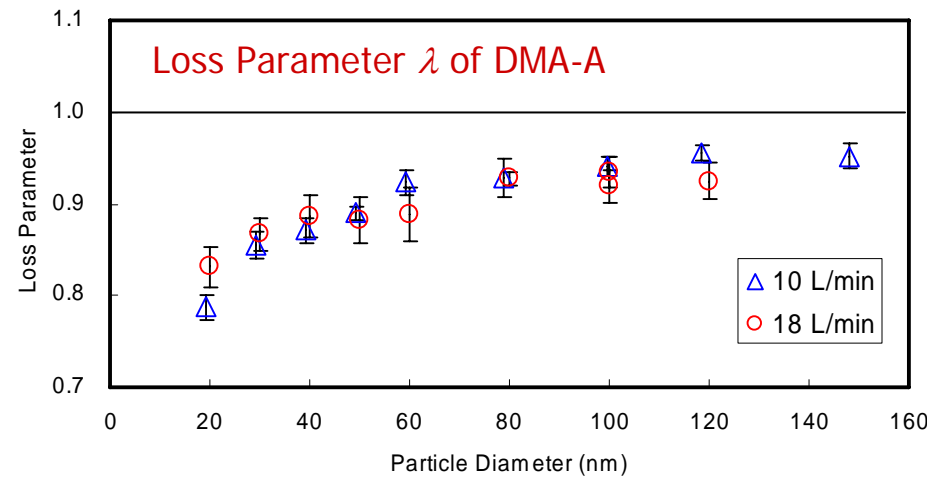
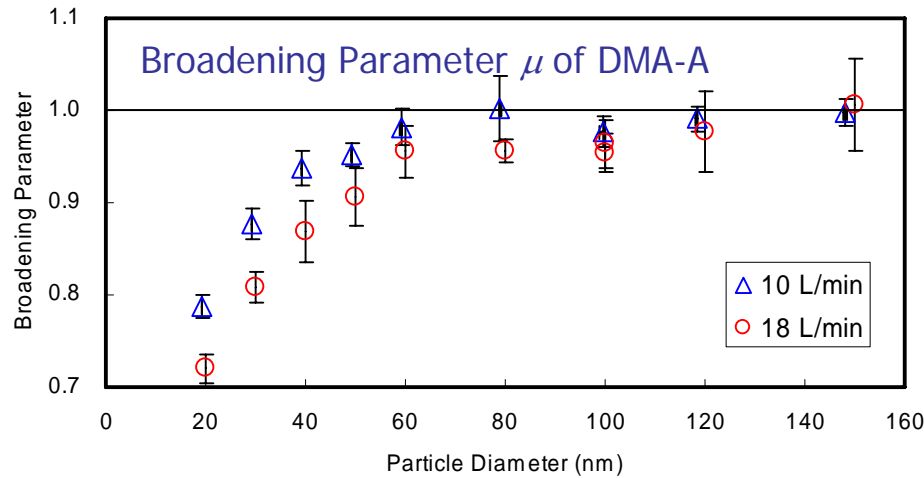
Results: Dependence on the Flow-Rate Ratio



	Average Broadening Parameter μ	Average Loss Parameter λ
A	0.996 (0.028)	0.937 (0.026)
B	0.983 (0.027)	0.938 (0.028)
C	0.994 (0.027)	0.931 (0.026)

- Neither broadening nor loss parameter showed apparent dependence on the flow-rate ratio.
- It was shown that, even at extreme settings such as Q_a and Q_s of 1 and 2 L/min ($Q_a/Q_s = 0.5$), the transfer function of the DMAs almost agreed with the theory.
- The standard deviations for the repeatability were as large as about 2-3%. We have not identified the source of these large scatterings.
- The broadening parameters averaged over the flow-rate ratio were in the range of 0.98-1.00 for the three DMAs, which means their resolutions were equal to the ideal.
- The averaged loss parameters were about 0.94, which means there were about 6% of loss in the DMA column.

Results: Dependence on Particle Size



- Above 60 nm, both broadening and loss parameters were essentially equal to the values at 100 nm. Below 50 nm, however, both parameters decreased as particle size decreased.
- Below 50 nm, the broadening parameter of 18 L/min was lower than that of 10 L/min.
- The size dependence of the loss parameter was fitted using the equation by Karlsson and Martinsson (2003):

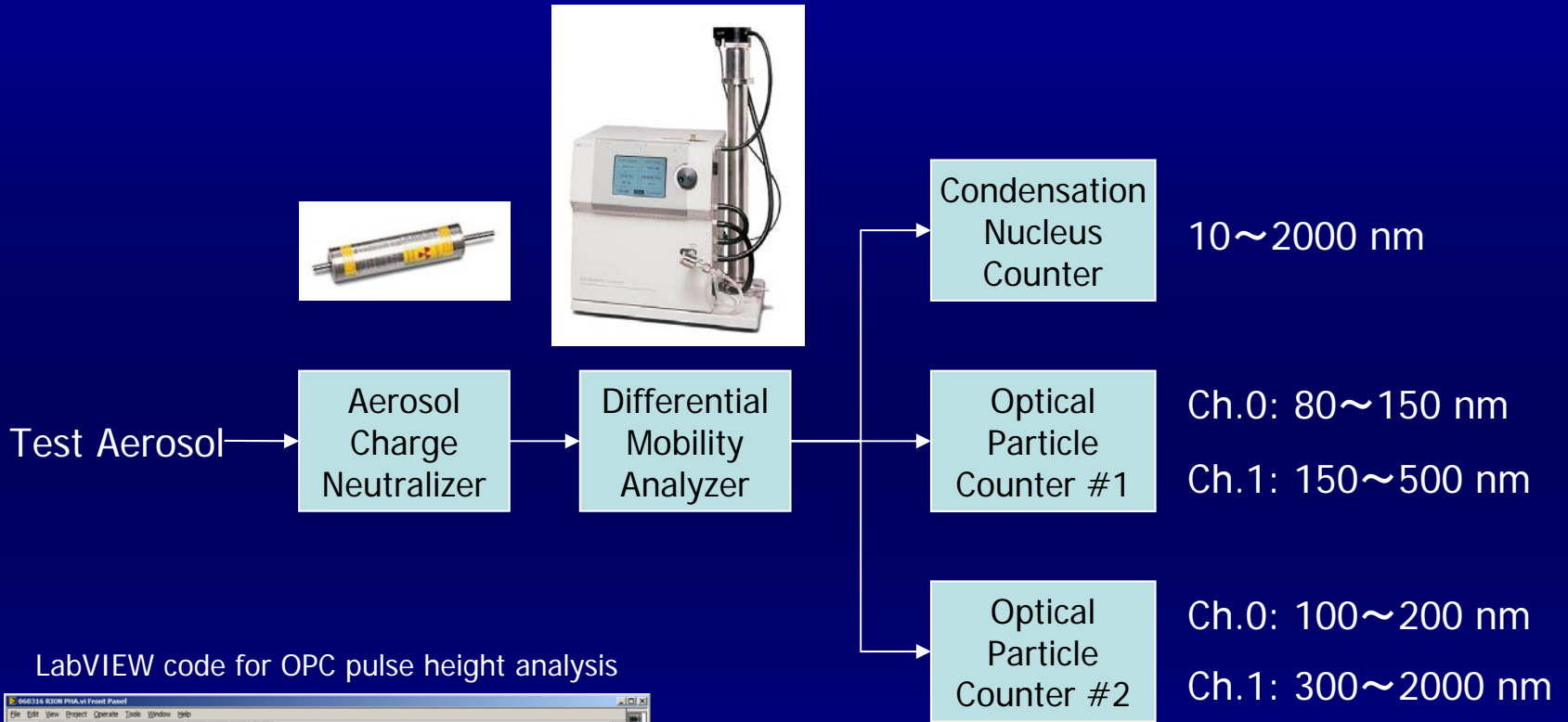
$$\lambda = \lambda_E \cdot \lambda_D(D_p, Q_a, L_{eff})$$

λ_E : losses due to electrostatic deposition, independent of particle size
 $\lambda_D(D_p, Q_a, L_{eff})$: losses due to diffusional deposition, dependent on particle size

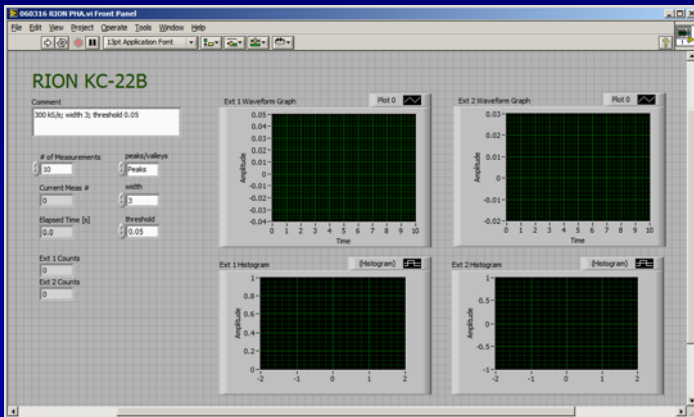
With the data of the 10-L/min sheath air flow rate, the parameters λ_E and L_{eff} were obtained for the three DMAs. While the λ_E parameter was very close to the value by Karlsson and Martinsson (2003), i.e., 0.98, the L_{eff} parameter was somewhat longer than their value (7.1 m).

	A	B	C	Average
λ_E [-]	0.971	0.966	0.961	0.97
L_{eff} [m]	9.51	10.20	9.14	9.6

AIST The Standard Reference Instrument of Size Distribution Measurement



LabVIEW code for OPC pulse height analysis



CNC

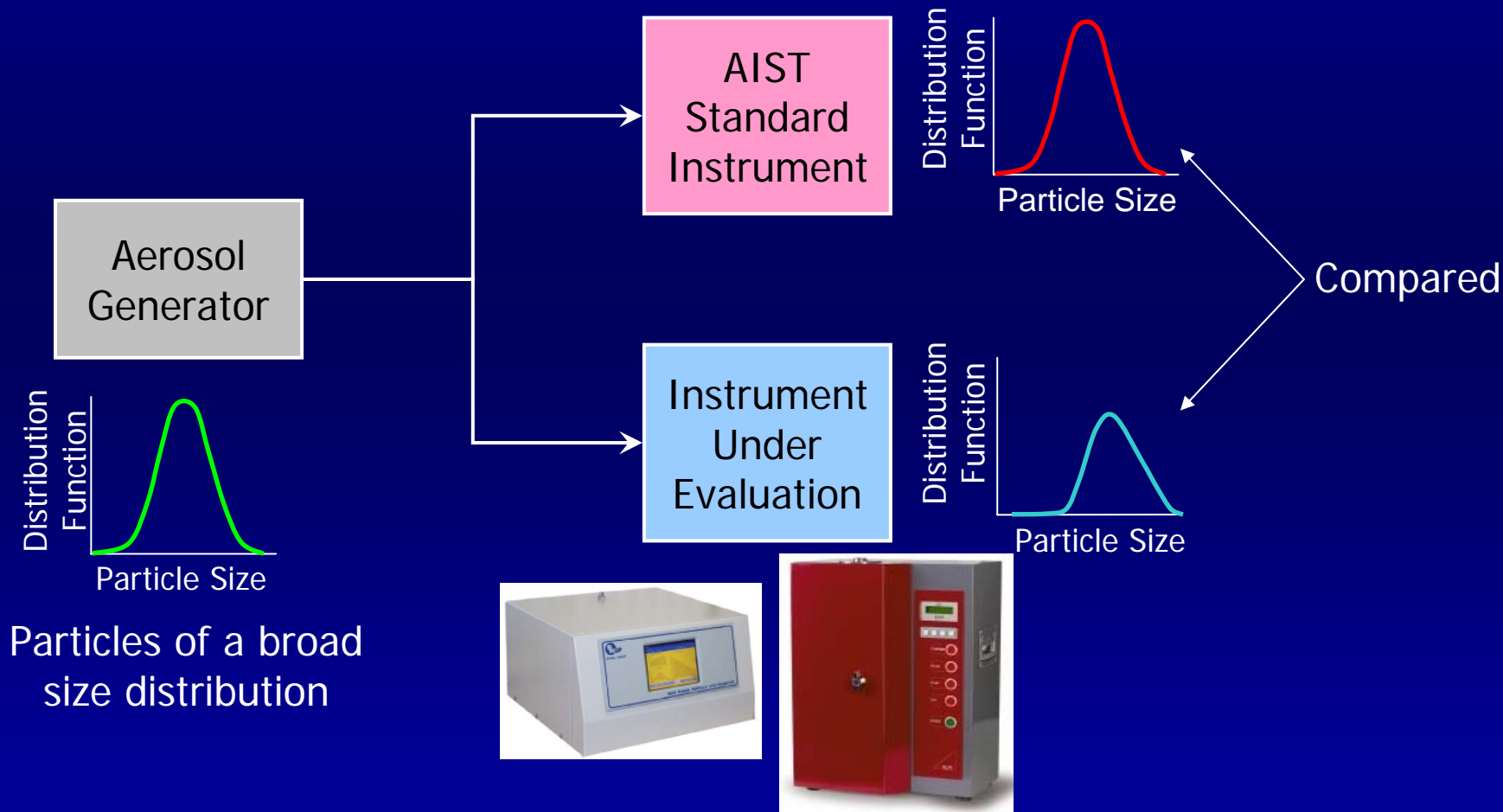


OPC1



OPC2

Test by Comparison to the Standard Reference Instrument



ISO on DMA/SEMS

ISO TC24 / SC 4 / WG 12

Committee Draft 15900

SEMS

“Determination of Particle Size Distribution — Differential Electrical Mobility Analysis for Aerosol Particles”

To be published as an International Standard by August 2008

“Validation and Calibration of Aerosol Particle Number Counters”

CNC

Approved as a Preliminary Work Item in April 2006

References

- Agarwal, J. K. and Sem, G. J. (1980). Continuous flow, single-particle-counting condensation nucleus counter. *J. Aerosol Sci.* 11, 343-357.
- Daire, A., Keithley Instruments, Inc. Article No. 2648, Counting electrons: How to measure currents in the attoampere range, September 2005.
- Karlsson, M. N. A., and Martinsson, B. G. (2003). Methods to measure and predict the transfer function size dependence of individual DMAs, *J. Aerosol Sci.* 34, 603-625.
- Knutson, E. O. and Whitby, K. T. (1975a). Aerosol classification by electric mobility: Apparatus, theory, and applications. *J. Aerosol Sci.* 6, 443-451.
- Knutson, E. O. and Whitby, K. T. (1975b). Accurate measurement of aerosol electric mobility moments, *J. Aerosol Sci.* 6, 453-460.
- Martinsson, B. G., Karlsson, M. N. A., and Frank, G. (2001). Methodology to estimate the transfer function of individual differential mobility analyzers, *Aerosol Sci. Technol.* 35, 815-823.
- Sakurai, H., Yabe, A., Takahata, K., and Ehara, K., Generation of sub-100 nm oil-droplet and PSL particles by electrospray, poster presented at the 7th International Aerosol Conference, September 2006.
- Wang, S. C. and Flagan, R. C. (1990). Scanning electrical mobility spectrometer. *Aerosol Sci. Technol.* 13, 230-240.
- Yun, C.-M., Otani, Y., and Emi, H. (1997). Development of unipolar ion generator - Separation of ions in axial direction of flow, *Aerosol Sci. Technol.* 26, 389-397.

hiromu.sakurai@aist.go.jp